1 **Efect of Potassium Hydroxide Concentration and Activation Time on Rice Husk-Activated Carbon**

2 **for Water Vapor Adsorption**

3 Dewi Qurrota A'yuni[1], Hadiantono[1], Velny[1], Agus Subagio[2], Moh. Djaeni[1,*] and Nandang Mufti[3]

4 *[1]Department of Chemical Engineering, Faculty of Engineering, Universitas Diponegoro*

5 *[2]Department of Physics, Faculty of Science and Mathematics, Universitas Diponegoro Jl. Prof. Soedarto*

6 *Tembalang, Semarang, Central Java, Indonesia 50275*

7 *[2]Department of Physics, Faculty of Mathematics and Scienc, Universitas Negeri Malang Jl. Semarang*

8 *No.5, Sumbersari, Lowokwaru, Malang, East Java 65145*

9 **Corresponding Author e-mail: moh.djaeni@live.undip.ac.id*

10

11 **Abstract:** Rice husk carbon by-product from the industrial combustion is a promising source to produce a

12 vast amount of activated carbon adsorbent. This research prepared rice husk-activated carbon adsorbent by

13 varying the concentration of potassium hydroxide solution (5, 10, 15, 20 % w/v) and activation time (2, 4,

14 6, 8 hours). Fourier-transform infrared spectral characterization (FTIR) indicated a significant effect before

15 and after activation, especially the presence of hydroxyl groups. Based on the iodine adsorption, the specific

16 surface area of the produced-activated carbon was approximately 615 m^2/g. Experimental results showed

17 that increasing potassium hydroxide concentration and activation time increases the water vapor adsorption

18 capacity of the activated carbon. Compared with the rice husk carbon, the KOH-activated carbon enhanced

19 the water vapor adsorption capacity to 931%. In the adsorption observation, changing the temperature from

20 15 to 27 °C caused a higher water vapor uptake onto the activated carbon. Two adsorption kinetics (pseudo-

21 first- and pseudo-second-order models) were used to evaluate the adsorption mechanism. This research

22 found that rice husk-activated carbon performed a higher water vapor adsorption capacity than other

23 adsorbents (silica gel, zeolite, and commercially activated carbon).

24 ***Keywords:*** *activated carbon, adsorption kinetics, desiccant, rice husk, water vapor adsorption*

25 **INTRODUCTION**

26 Water vapor adsorption is an essential process in several industrial practices, such as water harvesting [1],

27 dehumidification [2], and desalination. As an example, in the dehumidification drying process, reducing

28 water vapor from air enhances the driving force, which can shorten the drying time and retain heat-

29 sensitive ingredients in the food product [3]. This is due to the significant difference between the

30 concentration of water vapor on the food's surface and the air as the drying medium. Then, the mass

31 transfer of water vapor from the product to the air can be fastened.

32 The need for water vapor adsorption led to the production of efficient materials for moisture control.

33 Some studies presented different types of water adsorbents, including Covalent Organic Frameworks [4],

34 Metal-Organic Frameworks (MOFs) [5], zeolite [6], silica gel [7], mesoporous silica [8], and activated

35 carbon [9]. Covalent Organic Frameworks (COFs) and Metal-Organic Frameworks (MOFs) are mostly

36 used in the water harvesting process because of their remarkable adsorption properties, which are highly

37 tunable and high porosity [10]. However, those materials require careful handling due to potential

38 structural damage and complex synthesis processes, making them relatively higher cost compared to other

39 adsorbents [11]. Meanwhile, widely known water vapor adsorbents or desiccants (zeolite, silica gel, and

40 activated carbon) are easily regenerated and more stable in structure.

41 There are several requirements in the adsorbent selection, including toxicity, adsorption capacity, cycles,

42 and easiness in regeneration using low heat energy. Activated carbon is a non-toxic and thermally stable

43 adsorbent with a high water adsorption capacity due to its large surface area [12]. Also, activated carbon

44 can be produced from natural sources such as agricultural by-products. Thus, activated carbon is a

45 promising adsorbent due to its abundance, low cost, and potential for sustainable water vapor removal.

46 Rice husk is a natural adsorbent that has been applied for various applications, including heavy metal and

47 dye removal in wastewater [13], [14], CO_2 adsorption [2], and urine purification [15]. In its application as

48 a water vapor adsorbent, rice husk was exploited by Warsiki et al. [16] that produce rice husk-$CaCl_2$

49 composite desiccant. They reported that environmental humidity (water activity) and temperature

50 influenced the adsorption capacity of the adsorbent. However, the study did not compare rice husk-$CaCl_2$

51 adsorption with other adsorbents. Moreover, untreated rice husk still contains contaminants in its pores

52 and thus is still low in adsorption capacity. Another research showed that rice husk silica had the potential

53 as a silica gel substitute in water vapor adsorption [17]. The adsorption mechanism of rice husk silica and

54 silica gel was similar and affected by silanol groups on their surface. Nevertheless, commercial silica

55 adsorbed twice as much water vapor than silica produced from rice husk. Therefore, this research focuses

56 on synthesizing natural-based adsorbent with high water vapor adsorption.

57 This work aims to produce activated carbon from rice husk as a water vapor adsorbent and its comparison

58 with other commercial adsorbents (commercial activated carbon, silica gel, and zeolite). In the process,

59 several studies used potassium hydroxide, zinc chloride, hydrochloric acid, and sodium hydroxide as

60 activation agents to activate rice husk carbon [18], [19], [20]. In this study, potassium hydroxide (KOH)

61 was selected as the activation agent to increase the pore volume and adsorption capacity of the adsorbent

62 water vapor [21]. The activation agent concentration and the activation time were studied to assess the

63 water vapor adsorption property.

EXPERIMENTAL PROCEDURE

Materials

66 Rice husk char was bought from a local shop in Pedurungan, Semarang, Central Java. The char was sun-

67 dried before being activated. The experiment was conducted using potassium hydroxide (90% purity,

68 technical grade), hydrochloric acid (concentration of 32%, technical grade), distilled water, iodine solution

69 (concentration of 1%, Merck & Co., Inc.), sodium thiosulfate (98% purity, Merck & Co., Inc.), and

70 amylum (99% purity, Merck & Co., Inc.). Commercial adsorbents that were used as a comparison were

71 coal-based commercial activated carbon (size of 4 – 8 mesh), white silica gel (size of 2 – 4 mm), and

72 natural zeolite bought from a local shop (CV. Indrasari, Semarang, Central Java).

Carbon Activation

74 Before activation, rice husk char was prepared by pulverizing and sieving to 20 and 25 mesh. Char

75 activation was conducted by adding 25 grams of rice husk char to 150 mL of 5% w/v KOH solution and

76 letting it stand for 8 hours. The activated char (activated carbon) was filtered and washed using HCl and

77 distilled water until the washing solution achieved a neutral pH. The wet activated carbon was dried in an

78 oven at 110°C to the achievement of a constant mass and was placed in a desiccator. The activation

79 procedure was repeated using KOH solution at different concentrations (10, 15, and 20% w/v) and

80 activation times (2, 4, and 6 hours).

81 **Iodine Number Adsorption**

82 The iodine adsorption experiment was begun by mixing the activated carbon and 0.1 N iodine solution for

83 10 minutes. After the filtration, 10 mL of filtrate was titrated with 0.1 N sodium thiosulfate ($Na_2S_2O_3$)

84 until became light yellow. The solution was then titrated by 1% amylum until clear from the blue color.

85 The iodine adsorption capacity was calculated by the equation of (Suliestyah et al., 2020)

$$\text{Iodine number} = \frac{(V_1 N_1 - V_2 N_2)126.9 \times 5}{W} \tag{1}$$

86 with V_1 and V_2 are volume of iodine and sodium thiosulfate (mL), respectively, N_1 is the normality of

87 iodine (N), N_2 normality of sodium thiosulfate (N), and W is the mass of the sample (g).

88 **Adsorption capacity**

89 Fig. 1 describes the experimental setup of the adsorption test. The adsorption capacity of the produced

90 activated carbon was evaluated by placing 10 grams of activated carbon in an isolated mason jar.

91 Previously, the jar was filled with a specific amount of water. The adsorption capacity was the total mass

92 of water adsorbed into the sample that was measured by the gravimetric method. This test was conducted

93 under temperatures of 15 °C, room temperature (27 °C), and 40 °C for several days until equilibrium. In

94 comparison, several commercial adsorbents were also examined with iodine and water vapor adsorption.

95 The adsorption kinetics was evaluated using several models presented in Table 1. The adsorption capacity

96 of prepared activated carbon was then compared to other commercial adsorbents (commercial activated

97 carbon, natural zeolite, and silica gel).

98
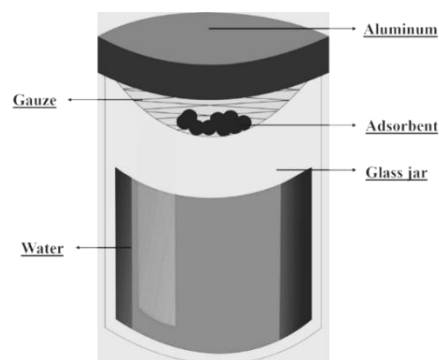
Fig. 1. Experimental set-up of the adsorption capacity evaluation

Table 1. Adsorption kinetics equation (Gurses et al. 2006; Qiu et al. 2009)

Model	Equation
Pseudo-first-order	$q_t = q_e(1 - e^{-k_1 t})$
Pseudo-second-order	$q_t = \dfrac{k_2 q_e{}^2 t}{1 + k_2 q_e t}$

Notes: q_t = moisture adsorption at a certain time; q_e = moisture adsorption at equilibrium; t = adsorption time; k_1 = constant parameter of pseudo-first-order; k_2 = constant parameter of pseudo-second-order

Materials Characterization

The functional groups in the activated carbon samples were examined using Fourier Transform Infrared

Spectroscopy (FTIR) employing PerkinElmer Frontier Infrared Spectrometer version 10.6.1, with a

resolution of 1 cm^{-1} in a region of 400 to 4000 cm^{-1}. X-ray diffractions (XRD PANalytical X'Pert PRO,

Malvern Panalytical Ltd.) with CuKα radiation of 1.54060Å were used to investigate the crystallinity of

natural zeolite. This instrument operated at 40 kV, 30 mA and the diffractograms were observed from

10.03° to 82.19° on a 2θ scale with a 0.7° step size. The chemical compositions of natural zeolite were

observed using X-ray Fluorescence (Panalytical Minipal 4, Malvern Panalytical Ltd.). Three random

samples were taken from the same source as the zeolite samples, named Zeolite A, B, and C. The crystal

structure and the chemical composition of natural zeolite were shown in XRD patterns and XRF analysis

in Fig. 2. According to XRD patterns evaluated by Highscore plus 3.0e (PANalytical B.V., The

Netherlands), the peaks of zeolite samples indicate similar crystal structure (mordenite). This result was

compatible with XRF analysis that showed a common compound of mordenite mineral (Na_2, Ca, K_2)

$Al_2Si_{10}O_{24} \cdot 7H_2O$ [22].

(a)

(b)
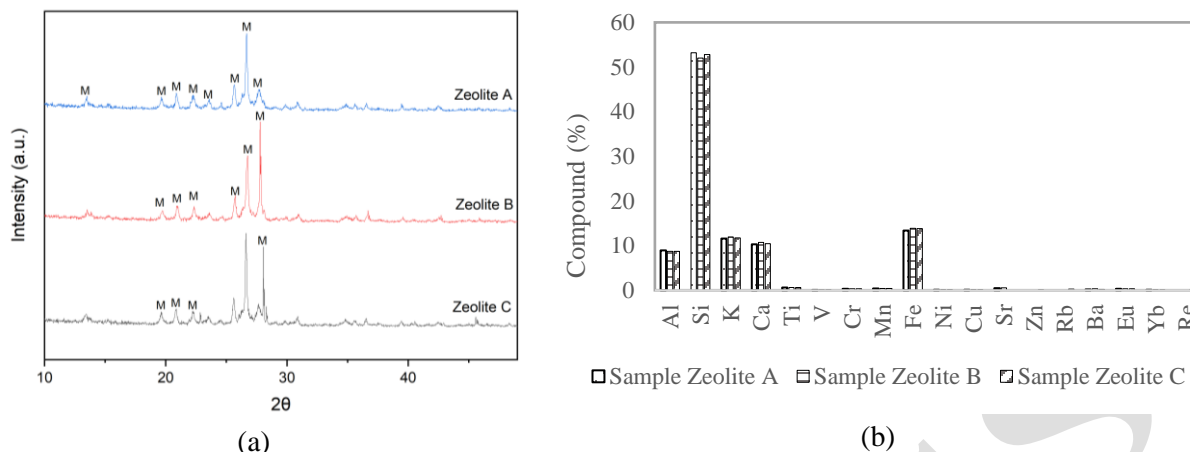
115   Fig. 2. (a) XRD patterns of natural zeolite used in this study (b) compounds found in natural zeolite used

116   in this study

Results and Discussion

Fourier transform infrared (FTIR) characterization

119   Fig. 3 shows the FTIR spectra of rice husk char and activated carbon, which highlight the chemical

120   functional groups. Several functional groups with water affinity were discovered by this characterization,

121   as well as some water that had bound to the activated carbon. A clear difference between the two samples

122   was a higher peak of aromatic ring C=C at $1600 - 1500$ cm^{-1} in the activated carbon and a C-O band of

123   rice husk char at $1300 - 1050$ cm^{-1} [23]. A C-H functional group at a wavenumber of 1374 cm^{-1}

124   corresponds to bending vibrations in methyl groups [24]. It also found a higher broad peak in the range of

125   wavenumber of $3600 - 3200$ cm^{-1}, representing the O-H functional group and indicating the moisture-

126   enriched surface of the activated carbon [13]. The oxygen-containing functional groups had the ability to

127   fasten the water vapor adsorption performance of the activated carbon [24].
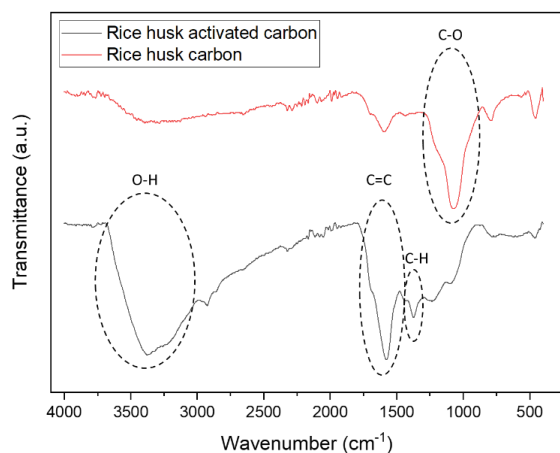
128

129   Fig. 3. FTIR spectra of rice husk char and activated carbon

130   **Iodine Adsorption**

131   According to Mianowski et al. [25], iodine adsorption can represent the surface area of activated carbon

132   for a range of 200 – 850 mg/g iodine number. Therefore, the surface area of rice husk activated carbon in

133   this study was around 615 m^2/g and higher than other tested commercial adsorbents (Fig. 4). According to

134   this result, the product can be potentially developed as a high-capacity water vapor adsorbent. However,

135   this result was still lower than nano-porous carbon with iodine adsorption of more than 700 mg/g [20].

136   This result indicates that the activated carbon product from this experiment had a higher lack of well-

137   developed porosity than that of nano-porous carbon from rice husk.
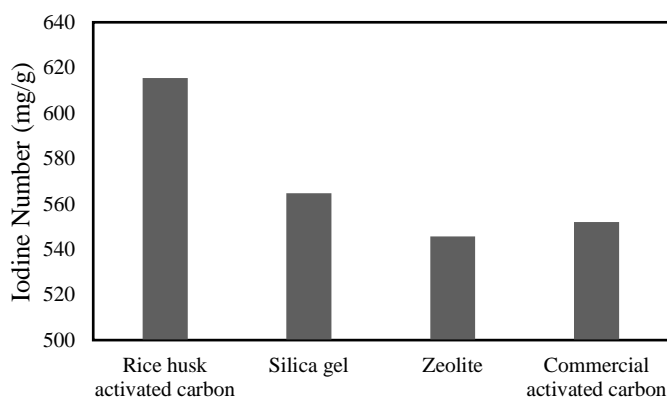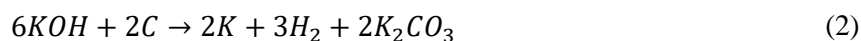

138

139   Fig. 4. Iodine adsorption of several adsorbents

140 **Effect of potassium hydroxide concentration**

141 In the activation stage, the chemical reaction that occurred was [26]

$$6KOH + 2C \rightarrow 2K + 3H_2 + 2K_2CO_3 \qquad (2)$$

142 Based on the reactions, KOH and carbon decomposed into potassium compounds (K and K_2CO_3) and

143 hydrogen. The activated carbon was then washed with acid and water to remove them, clearing carbon

144 pores [27]. Therefore, the water vapor adsorption of carbon was increased after the activation (Fig. 5).

145 Untreated rice husks possessed the lowest adsorption capacity (0.04 g water/g adsorbent). Fig. 5 also

146 presents water vapor adsorption of the activated carbon that was treated using different KOH

147 concentrations for 8 hours. The data shows that manufacturing activated carbon using higher KOH

148 concentration impacted a higher adsorption capacity. The highest adsorption capacity (0.42 g vapor/g

149 adsorbent) belonged to activated carbon obtained from activation using 20% w/v KOH solution, and the

150 lowest was found at 5% w/v KOH solution.

151 This finding confirmed the FTIR characterization that showed a hydroxyl functional group on the

152 activated carbon. Also, the theory stated that a higher activation agent concentration facilitates higher

153 carbon degradation to produce more pores [28]. However, the produced activated carbon was still lower

154 than activated carbon derived from coffee shells [24] and tobacco stems [29]. The significance of different

155 concentrations and adsorption times were evaluated with ANOVA summarized in Table 2, showing a

156 significant impact of both factors (p-value < 0.05).
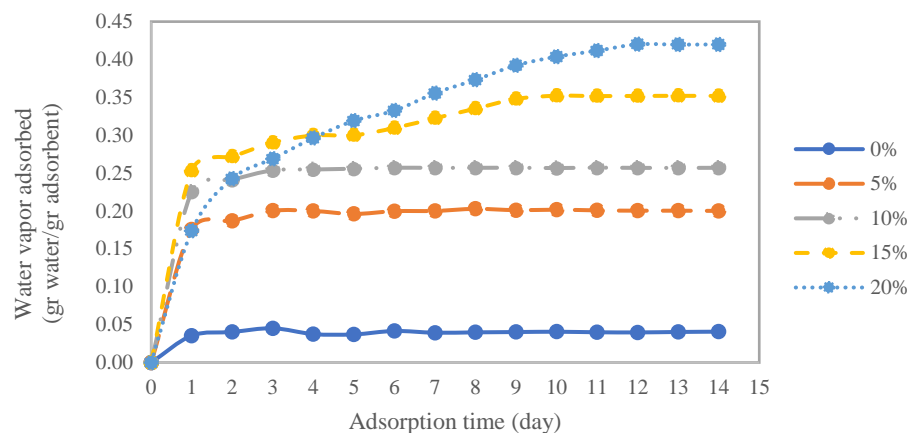
Fig. 5. Water vapor adsorption of activated carbon at different concentrations

Table 2. Two-way ANOVA of water vapor adsorption of the activated carbon at different adsorption times and KOH concentrations
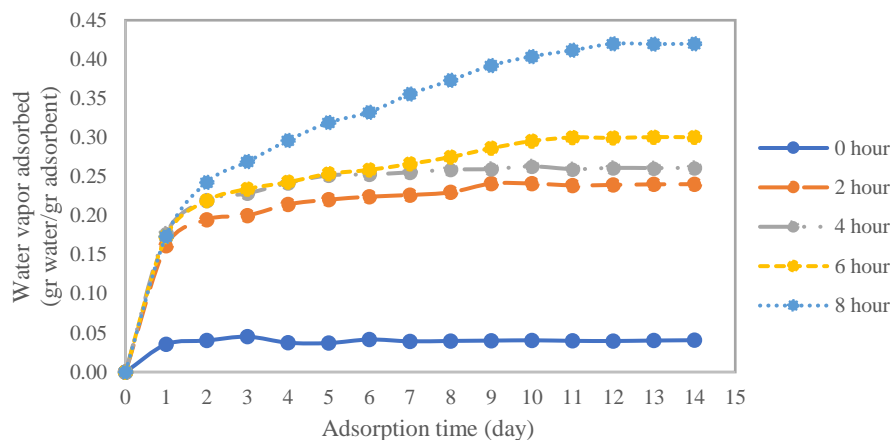
Source of Variation	SS	df	MS	F	*P-value*	F crit
Adsorption time	28.9739	14	2.0696	10.7222	< 0.001	1.8726
Concentration	77.3276	4	19.3319	100.1570	< 0.001	2.5366
Error	10.8089	56	0.1930			
Total	117.1103	74				

Effect of Activation Time

The analysis of the activation time was conducted for activated carbon that was activated using 20% w/v

KOH solution for 2 – 8 hours. Fig. 6 depicts the adsorption capacity at different activation times. The

highest adsorption capacity was achieved at 8 hours of carbon activation (0.420 g vapor adsorbed/g

adsorbent). Compared to the untreated rice husk char, activating the carbon for 8 hours increased the

adsorption capacity up to 9 times. Analysis of the variance of this result also demonstrated that varying the

activation period has a significant effect on the adsorption capacity (Table 3).

Previous studies reported a different relationship between the activation time and adsorption capacity [24],

[28]. Sun et al. [24] stated that changes in activation time did not have a significant effect on the

maximum adsorption capacity. In contrast, Yang et al. [28] found a fluctuation in the adsorption capacity

of activated carbon at different activation times. From a range of 0.5 to 3.0 hours, the maximum

methylene blue adsorption was at 2 hours. That result occurred because of an excessive increase in

173   reaction rate between KOH and carbon causing a higher growth of porous structure. Extending the

174   activation duration can increase the contaminants degradation and maximize the microporous formation

175   [30].

176

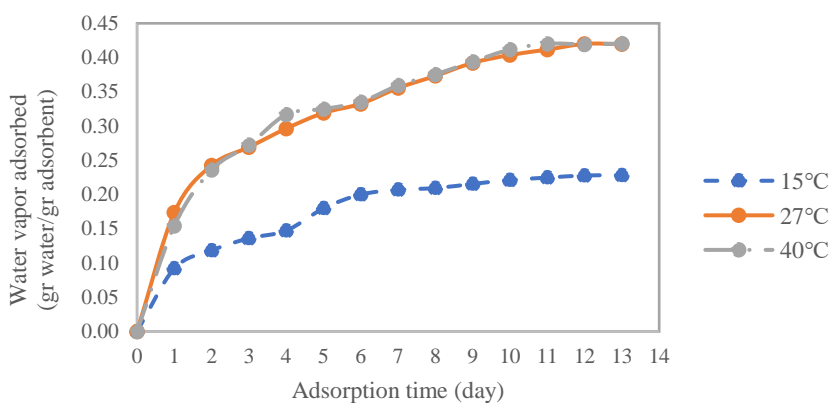177   Fig. 6. Water vapor adsorption capacities at different activation times

178   Table 3. Two-way ANOVA of water vapor adsorption of the activated carbon at different activation times

Source of Variation	SS	df	MS	F	*P-value*	F crit
Adsorption time	30.0561	14	2.1469	13.3901	< 0.001	1.8726
Activation time	66.2628	4	16.5657	103.3209	< 0.001	2.5366
Error	8.9786	56	0.1603			
Total	105.2976	74				

179   **Effect of Adsorption Temperature**

180   The effect of adsorption temperature on the water vapor adsorption capacity of activated carbon was

181   presented in Fig. 7. The test observed that a change of temperature of 15 °C to 27 °C affected the

182   adsorption capacity. At 40 °C, there was no significant difference in the maximum water vapor adsorption

183   capacity. More details, ANOVA indicated that the adsorption temperature and time had a significant effect

184   on the water vapor adsorption (Table 4). Before, Chairunnisa et al. [12] and Cardenas et al. [31] explored

185   the water vapor adsorption of activated carbon at 20 - 40°C. They found that increasing the adsorption

186   temperature caused a reduction in the adsorption capacity. Combined with our results, the phenomenon

187   that happened was a rapid formation of water clusters at temperatures lower than 30°C, and at higher

188 temperatures, this water cluster became less stable [12]. Higher temperatures sped up the movement of

189 water molecules and reduced the attraction of adsorbent and water [32].

190

191 Fig. 7. Water vapor adsorption capacity at different temperatures

192 Table 4. Two-way ANOVA of water vapor adsorption capacity of the activated carbon at different

193 temperatures

Source of Variation	SS	df	MS	F	*P-value*	F crit
Time	0.3975	13	0.0306	31.5170	< 0.001	2.1192
Temperature	0.1939	2	0.0970	99.9622	< 0.001	3.3690
Error	0.0252	26	0.0010			
Total	0.6166	41				

194

195 Fig. 8 displays the effect of the adsorption temperature of several adsorbents. Interestingly, different

196 adsorbents exhibited a different relationship. For example, when the temperature increased from 15 °C to

197 40 °C, the maximum adsorption capacity of commercial activated carbon decreased by 33%. Furthermore,

198 the adsorption capacity of other adsorbents increased when the temperature increased from 15°C to 40°C.

199 Also, this comparison indicated that the produced activated carbon from rice husk adsorbed more water

200 vapor than other tested commercial adsorbents. This result was in agreement with the iodine adsorption

201 test that showed a higher surface area of rice husk-activated carbon than other adsorbents.
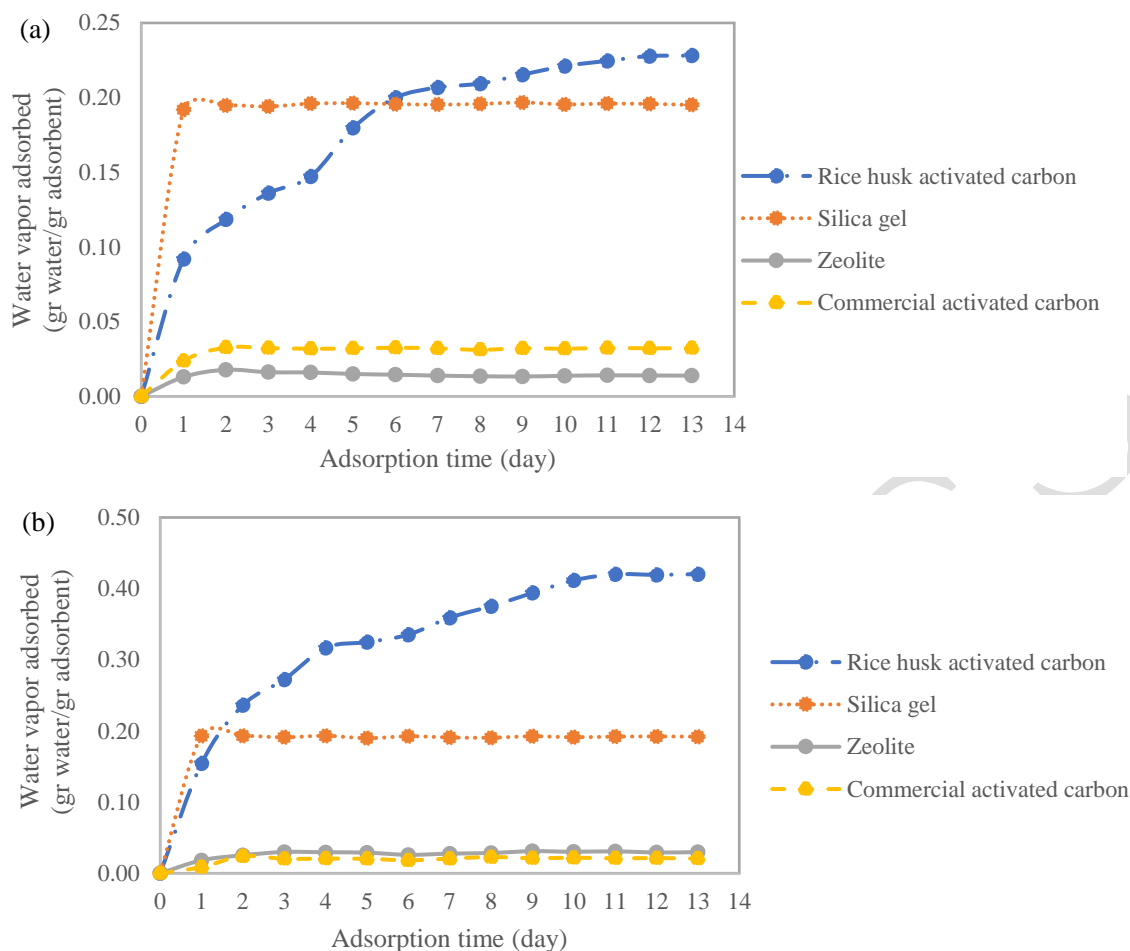
202

203

204 Fig. 8. Water vapor adsorption of several adsorbents at temperatures of (a) 15°C, (b) 40°C

205 **Adsorption Kinetics**

206 The adsorption kinetics of prepared activated carbon (20% w/v KOH solution and 8 hours activation) was

207 evaluated by pseudo-first- and pseudo-second-order models. The kinetic study was analyzed by varying

208 the adsorption temperature at 15 °C, 27 °C, and 40 °C. The parameters of the two models are provided in

209 Table 5. The most suitable model was determined by coefficient of determination (R^2) and SSE. Based on

210 the calculation, two models show good fits with R^2 close to 1.0 and SSE close to 0. Furthermore, the

211 pseudo-first-order model described the adsorption mechanism of activated carbon prepared at the highest

212 concentration and longest activation time was better than the second-order (R^2 values closer to 1 and SSE

213 closer to 0). It implied that the main mechanism for the adsorption of water vapor on that activated carbon

214 was physisorption. Meanwhile, the pseudo-second-order model described some samples better than the

215   first-order, agreeing to the chemisorption process [33].

216   Table 5. Parameters of non-linear pseudo-first- and pseudo-second-order model

Concentration (% w/v)	Pseudo-First-Order				Pseudo-Second-Order			
	k_1	q_e	R^2	SSE	k_2	q_e	R^2	SSE
5	0.0013	0.2001	0.8383	9.6×10^{-6}	0.0240	0.2001	0.8921	1.9×10^{-5}
10	0.0009	0.2572	0.9396	6.3×10^{-5}	0.0714	0.2569	0.9551	4.5×10^{-5}
15	0.0005	0.3506	0.6702	0.0008	0.0034	0.3506	0.8340	0.0002
20	0.0002	0.4184	0.9618	0.0006	0.0012	0.4184	0.9492	0.0007
Activation time (hour)								
2	0.0003	0.2405	0.9614	0.0006	0.0078	0.2405	0.9561	6.0×10^{-5}
4	0.0003	0.2656	0.9864	0.0008	0.0062	0.2656	0.9905	3.0×10^{-5}
6	0.0003	0.3013	0.8805	0.0005	0.0031	0.3013	0.9309	0.0001
8	0.0002	0.4184	0.9613	0.0006	0.0010	0.4184	0.9532	0.0008
Temperature (°C)								
15	0.0002	0.2326	0.9686	0.0001	0.0019	0.2326	0.9398	0.0003
27	0.0002	0.4184	0.9613	0.0006	0.0010	0.4184	0.9532	0.0008
40	0.0003	0.4224	0.9425	0.0007	0.0009	0.4224	0.9772	0.0011

217   **CONCLUSION**

218   Activated carbon from rice husks was activated by varying the concentration of KOH as the activation

219   agent and the activation time. The Fourier transform infrared (FTIR) spectral characterization represents

220   that there was a significant effect on the activation of rice husk activated carbon as indicated by

221   differences in functional groups before and after activation, including the addition of the hydroxyl group

222   which made the activated carbon more hydrophilic, and the presence of the C=C group indicated an

223   increase in carbon content. Based on the iodine adsorption test, the surface area of the activated carbon

224   produced was around 615 m^2/g. The adsorption test showed that an increase in KOH concentration of up

225   to 20% (w/v) and an activation time of 8 hours could increase the adsorption capacity of the resulting

226   activated carbon (up to 0.420 g/g). Adsorption was also examined at 15°C, 27 °C, and 40 °C and showed

227   an increase in adsorption capacity with increasing temperature. The produced activated carbon that was

228   activated using 20% w/v KOH for 8 hours showed a good fit with the pseudo-first-order adsorption

229   kinetics model. According to the comparison, activated carbon from rice husk showed a higher adsorption

230 capacity than silica gel, zeolite, and commercial activated carbon. This research found that activated

231 carbon from rice husks is a promising material to be applied to the dehumidification system of a drying

232 process.

233 **ACKNOWLEDGEMENT**

235 **REFERENCES**

236 [1] Sleiti, A. K., Al-Khawaja, H., Al-Khawaja, H. and Al-Ali, M., "*Harvesting Water from Air Using*

237 *Adsorption Material – Prototype and Experimental Results.*" *Sep. Purif. Technol.*, 2021, 257,

238 117921.

239 [2] Wang, C., Yang, B., Ji, X., Zhang, R. and Wu, H., "*Study on Activated Carbon/Silica Gel/Lithium*

240 *Chloride Composite Desiccant for Solid Dehumidification.*" *Energy*, 2022, 251, 123874.

241 [3] Djaeni, M. and Perdanianti, A. M., "*The Study Explores the Effect of Onion (Allium Cepa L.)*

242 *Drying Using Hot Air Dehumidified by Activated Carbon, Silica Gel and Zeolite.*" *J. Phys.: Conf.*

243 *Ser.*, 2019, 1295, 012025.

244 [4] Xia, X., Liu, Z. and Li, S., "*Adsorption Characteristics and Cooling/Heating Performance of COF-*

245 *5.*" *Appl. Therm. Eng.*, 2020, 176, 115442.

246 [5] Ashraf, S., Sultan, M., Bahrami, M., McCague, C., Shahzad, M. W., Amani, M., Shamshiri, R. R.

247 and Ali, H. M., "*Recent Progress on Water Vapor Adsorption Equilibrium by Metal-Organic*

248 *Frameworks for Heat Transformation Applications.*" *Int. Commun. Heat and Mass Transf.*, 2021,

249 124, 105242.

250 [6] Moura, P. A. S., Rodríguez-Aguado, E., Maia, D. A. S., Melo, D. C., Singh, R., Valencia, S.,

251 Webley, P. A., Rey, F., Bastos-Neto, M., Rodríguez-Castellón, E. and Azevedo, D. C. S., "*Water*

252 *Adsorption and Hydrothermal Stability of CHA Zeolites with Different Si/Al Ratios and*

253 *Compensating Cations.*" *Catal. Today*, 2022, 390–391, 99–108.

254 [7]   Zheng, X., Chen, K. and Lin, Z., "*Synthesis and Characterization of Alginate–Silica Gel*

255   *Composites for Adsorption Dehumidification*." *Ind. Eng. Chem. Res.*, 2020, 59, 5760–5767.

256 [8]   A'yuni, D. Q., Subagio, A., Hadiyanto, H., Kumoro, A. C. and Djaeni, M., "*Microstructure Silica*

257   *Leached by NaOH from Semi-Burned Rice Husk Ash for Moisture Adsorbent*." *Arch. Mater. Sci.*

258   *Eng.*, 2021, 1, 5–15.

259 [9]   Sun, S., Yu, Q., Li, M., Zhao, H., Wang, Y. and Ji, X., "*Effect of Carbonization Temperature on*

260   *Characterization and Water Vapor Adsorption of Coffee-Shell Activated Carbon*." *Ads. Sci.*

261   *Technol.*, 2020, 38, 377–392.

262 [10] Zu, K. and Qin, M., "*Experimental and Modelling Investigation of Water Adsorption of Hydrophilic*

263   *Carboxylate-Based MOF for Indoor Moisture Control*." *Energy*, 2021, 228, 120654.

264 [11] Gargiulo, N., Peluso, A. and Caputo, D., "*MOF-Based Adsorbents for Atmospheric Emission*

265   *Control: A Review*." *Processes*, 2020, 8, 613.

266 [12] Chairunnisa, Miksik, F., Miyazaki, T., Thu, K., Miyawaki, J., Nakabayashi, K., Wijayanta, A. T.

267   and Rahmawati, F., "*Development of Biomass Based-Activated Carbon for Adsorption*

268   *Dehumidification*." *Energy Rep.*, 2021, 7, 5871–5884.

269 [13] Liu, Z., Sun, Y., Xu, X., Qu, J. and Qu, B., "*Adsorption of Hg(II) in An Aqueous Solution by*

270   *Activated Carbon Prepared from Rice Husk Using KOH Activation*." *ACS Omega*, 2020, 5, 45,

271   29231–29242.

272 [14] Wazir, A. H., Ullah, I. and Yaqoob, K., "*Chemically Activated Carbon Synthesized from Rice Husk*

273   *for Adsorption of Methylene Blue in Polluted Water*." *Environ. Eng. Sci.*, 2023, 40, 307–317.

274 [15] Sintawardani, N., Adhilaksma, C. A., Hamidah, U., Pradanawati, S. A. and Suharno, S. M.,

275   "*Evaluation of Human Urine Purification Using Rice Husk Charcoal as The Adsorbent*." *IOP Conf.*

276   *Ser.: Earth Environ. Sci.*, 2023, 1201, 012107.

277 [16] Warsiki, E., Agriawati, D., Noor, E. and Iskandar, A., "*Isotherm Moisture Sorption of Composite*

278   *Desiccant Made from Rice Husk Biomass*." *IOP Conf. Ser.: Earth Environ. Sci.*, 2021, 749, 012011.

279 [17] Chirsty, A. A. and Sivarukshy, P., "*Comparison of Adsorption Properties of Commercial Silica and*

280   *Rice Husk Ash (RHA) Silica: A Study by NIR Spectroscopy,*" *Open Chem.*, 2021, 19, 426–431.

281 [18] Emdadi, Z., Asim, N., Yarmo, M. A, Ebadi, M., Mohammad, M. and Sopian, K., "*Chemically*

282   *Treated Rice Husk Blends as Green Desiccant Materials for Industrial Application.*" *Chem. Eng.*

283   *Technol.*, 2017, 40, 1619–1629.

284 [19] He, S., Chen, G., Xiao, H., Shi, G., Ruan, C., Ma, Y., Dai, H., Yuan, B., Chen, X. and Yang., X.,

285   "*Facile Preparation of N-Doped Activated Carbon Produced from Rice Husk for CO_2 Capture.*" *J.*

286   *Colloid Interface Sci.*, 2021, 582, 90–101.

287 [20] Shrestha, L., Thapa, M., Shrestha, R., Maji, S., Pradhananga, R. and Ariga, K., "*Rice Husk-Derived*

288   *High Surface Area Nanoporous Carbon Materials with Excellent Iodine and Methylene Blue*

289   *Adsorption Properties.*" *C*, 2019, 5, 10.

290 [21] Liu, Y., Huo, Z., Song, Z., Zhang, C., Ren, D., Zhong, H. and Jin, F., "*Preparing a Magnetic*

291   *Activated Carbon with an Expired Beverage as Carbon Source and KOH as The Activator.*" *J.*

292   *Taiwan Inst. Chem. Eng.*, 2019, 96, 575–587.

293 [22] Philia, J., Widayat, W., Sulardjaka, S., Nugroho, G. A. and Darydzaki, A. N., "*Aluminum-Based*

294   *Activation of Natural Zeolite for Glycerol Steam Reforming.*" *Results Eng.*, 2023, 19, 101247.

295 [23] Muslim, A., Purnawan, E., Meilina, H., Azwar, M. Y., Deri, N. O. and Kadri, A., "*Adsorption of*

296   *Copper Ions onto Rice Husk Activated Carbon Prepared Using Ultrasound Assistance:*

297   *Optimization Based on Step-by-Step Single Variable Knockout Technique.*" *J. Eng. Sci. Technol.*,

298   2022, 17, 2496–2511.

299 [24] Sun, S., Yu, Q., Li, M., Zhao, H. and Wu, C., "*Preparation of Coffee-Shell Activated Carbon and*

300   *Its Application for Water Vapor Adsorption.*" *Renew. Energy*, 2019, 142, 11–19.

301 [25] Mianowski, A., Owczarek, M. and Marecka, A., "*Surface Area of Activated Carbon Determined by*

302   *the Iodine Adsorption Number.*" *Energy Sources*, Part A: Recovery, Utilization, and Environmental

303   Effects, 2007, 29, 839–850.

304 [26] Linares-Solano, A., Lillo-Ródenas, M. A., Marco-Lozar, J. P., Kunowsky, M. and Romero-Anaya,

305 A. J., "*Naoh and KOH for Preparing Activated Carbons Used in Energy and Environmental*

306 *Applications.*" *Int. J. Energy*, Environment and Economics, 2012, 20, 59–91.

307 [27] Oginni, O., Singh, K., Oporto, G., Dawson-Andoh, B., McDonald, L. and Sabolsky, E., "*Influence*

308 *of One-Step and Two-Step KOH Activation on Activated Carbon Characteristics.*" *Bioresour.*

309 *Technol. Rep.*, 2019, 7, 100266.

310 [28] Yang, H. M., Zhang, D. H., Chen, Y., Ran, M. J. and Gu, J. C., "*Study on The Application of KOH*

311 *to Produce Activated Carbon to Realize the Utilization of Distiller's Grains*." *IOP Conf. Ser: Earth*

312 *Environ. Sci.*, 2017, 69.

313 [29] Yu, Q., Zhao, H., Zhao, H., Sun, S., Ji, X., Li, M. and Wang, Y., "*Preparation of Tobacco-Stem*

314 *Activated Carbon from Using Response Surface Methodology and Its Application for Water Vapor*

315 *Adsorption in The Solar Drying System.*" *Sol. Energy*, 2019, 177, 324–336.

316 [30] Liang, Q., Liu, Y., Chen, M., Ma, L., Yang, B., Li, L. and Liu, Q., "*Optimized Preparation of*

317 *Activated Carbon from Coconut Shell and Municipal Sludge.*" *Mater. Chem. Phys.*, 2020, 241,

318 122327.

319 [31] Cardenas, C., Farrusseng, D., Daniel, C. and Aubry, R., "*Modeling of Equilibrium Water Vapor*

320 *Adsorption Isotherms on Activated Carbon, Alumina and Hoplite.*" *Fluid Phase Equilib.*, 2022, 561,

321 113520.

322 [32] Wang, T., Tian, S., Li, G., Sheng, M., Ren, W., Liu, Q., Tan, Y. and Zhang, P., "*Experimental Study*

323 *of Water Vapor Adsorption Behaviors on Shale.*" *Fuel*, 2019, 248, 168–177.

324 [33] Robati, D., "*Pseudo-Second-Order Kinetic Equations for Modelling Adsorption Systems for*

325 *Removal of Lead Ions Using Multi-Walled Carbon Nanotube,*" *J. Nanostruct. Chem.*, 2013, 3, 55.

326